



Aalborg Universitet

AALBORG UNIVERSITY
DENMARK

Resistance to vincristine in DLBCL by disruption of p53-induced cell cycle arrest and apoptosis mediated by KIF18B and USP28

Rovsing, Anne Bruun; Thomsen, Emil Aagaard; Nielsen, Ian; Skov, Thomas Wisbech; Luo, Yonglun; Dybkær, Karen; Mikkelsen, Jacob Giehm

Published in:
British Journal of Haematology

DOI (link to publication from Publisher):
[10.1111/bjh.18872](https://doi.org/10.1111/bjh.18872)

Creative Commons License
CC BY-NC 4.0

Publication date:
2023

Document Version
Publisher's PDF, also known as Version of record

[Link to publication from Aalborg University](#)

Citation for published version (APA):

Rovsing, A. B., Thomsen, E. A., Nielsen, I., Skov, T. W., Luo, Y., Dybkær, K., & Mikkelsen, J. G. (2023). Resistance to vincristine in DLBCL by disruption of p53-induced cell cycle arrest and apoptosis mediated by KIF18B and USP28. *British Journal of Haematology*, 202(4), 825-839. <https://doi.org/10.1111/bjh.18872>

General rights

Copyright and moral rights for the publications made accessible in the public portal are retained by the authors and/or other copyright owners and it is a condition of accessing publications that users recognise and abide by the legal requirements associated with these rights.

- Users may download and print one copy of any publication from the public portal for the purpose of private study or research.
- You may not further distribute the material or use it for any profit-making activity or commercial gain
- You may freely distribute the URL identifying the publication in the public portal -

Take down policy

If you believe that this document breaches copyright please contact us at vbn@aub.aau.dk providing details, and we will remove access to the work immediately and investigate your claim.

ORIGINAL PAPER

Resistance to vincristine in DLBCL by disruption of p53-induced cell cycle arrest and apoptosis mediated by KIF18B and USP28

Anne Bruun Roving¹  | Emil Aagaard Thomsen¹  | Ian Nielsen¹ | Thomas Wisbech Skov¹ | Yonglun Luo^{1,2}  | Karen Dybkær³ | Jacob Giehm Mikkelsen¹ 

¹Department of Biomedicine, Aarhus University, Aarhus, Denmark

²Lars Bolund Institute of Regenerative Medicine, BGI-Qingdao, BGI-Shenzhen, Shenzhen, China

³Department of Hematology, Aalborg University Hospital, Aalborg, Denmark

Correspondence

Jacob Giehm Mikkelsen, Høegh-Guldbergs Gade 10, 8000 Aarhus C, Denmark.
 Email: giehm@biomed.au.dk

Funding information

Andersen-Isted Fonden; Dagmar Marshalls Fond; Danmarks Frie Forskningsfond; Direktør Jacob Madsens og Olga Madsens Fond; Fabrikant Einar Willumsens Mindelegat; Helga og Peter Kornings Fond; NEYE-Fonden; Ny Carlsbergfondet; Raimond og Dagmar Ringgård-Bohns Fond

Summary

The frontline therapy R-CHOP for patients with diffuse large B-cell lymphoma (DLBCL) has remained unchanged for two decades despite numerous Phase III clinical trials investigating new alternatives. Multiple large studies have uncovered genetic subtypes of DLBCL enabling a targeted approach. To further pave the way for precision oncology, we perform genome-wide CRISPR screening to uncover the cellular response to one of the components of R-CHOP, vincristine, in the DLBCL cell line SU-DHL-5. We discover important pathways and subnetworks using gene-set enrichment analysis and protein–protein interaction networks and identify genes related to mitotic spindle organization that are essential during vincristine treatment. The inhibition of KIF18A, a mediator of chromosome alignment, using the small molecule inhibitor BTB-1 causes complete cell death in a synergistic manner when administered together with vincristine. We also identify the genes *KIF18B* and *USP28* of which CRISPR/Cas9-directed knockout induces vincristine resistance across two DLBCL cell lines. Mechanistic studies show that lack of *KIF18B* or *USP28* counteracts a vincristine-induced p53 response suggesting that resistance to vincristine has origin in the mitotic surveillance pathway (USP28–53BP1–p53). Collectively, our CRISPR screening data uncover potential drug targets and mechanisms behind vincristine resistance, which may support the development of future drug regimens.

KEY WORDS

cancer, CHOP, CRISPR/Cas9, drug resistance, lymphomas, p53

INTRODUCTION

Only around 65% of diffuse large B-cell lymphoma (DLBCL) patients are cured after treatment with the frontline regimen R-CHOP consisting of the anti-CD20 antibody rituximab, three chemotherapeutics (cyclophosphamide, doxorubicin and vincristine), and the immuno-suppressive steroid prednisone.¹ To improve the treatment outcome, several changes of the R-CHOP regimen have been tested in phase III clinical trials including dose intensification, substitution of antibodies, and the addition of novel agents such as ibrutinib, lenalidomide and bortezomib.² Unfortunately, this has not

led to significant improvements. Recently, the POLARIX phase III trial comparing R-CHOP to Pola-R-CHP, in which vincristine was substituted with polatuzumab vedotin, a CD79b-targeting antibody-drug conjugate, showed higher progression-free survival after 2 years.³ However, the trial showed no difference in overall survival, and regulatory approval of this regimen has not yet been granted. Following initiation of these clinical trials, three recent studies characterized new genetic DLBCL subtypes using among other DNA sequencing to identify recurrent genetic alterations in large DLBCL patient cohorts.^{4–6} These new genetic subtypes share considerable overlaps, suggesting that they are rooted

This is an open access article under the terms of the [Creative Commons Attribution-NonCommercial](https://creativecommons.org/licenses/by-nc/4.0/) License, which permits use, distribution and reproduction in any medium, provided the original work is properly cited and is not used for commercial purposes.

© 2023 The Authors. *British Journal of Haematology* published by British Society for Haematology and John Wiley & Sons Ltd.

in biologically meaningful distinctions valuable for designing future clinical trials.

Vincristine has been widely used in the first-line treatment of blood, brain, bone and kidney cancers among others since the 1960s.⁷ Vincristine interferes with mitosis by binding β -tubulin, which disrupts the capacity of microtubules to separate chromosomes during metaphase. This halts proliferating cells at the spindle assembly checkpoint (SAC) until the cells resolve the mitotic spindle disruption or the prolonged SAC causes apoptosis. Cells may also exit the SAC prematurely causing chromosome mis-segregation, which results in aneuploid cells, after which either cell cycle arrest, apoptosis or chromosome instability is seen. Despite the many years of use and extensive research into the mechanism of action and toxic side effects, it remains uncertain why some patients do not benefit from vincristine treatment and why resistance to vincristine occurs.^{8,9}

Genome-wide genetic screening using CRISPR/Cas9-based technologies enables unbiased identification of genes altering cellular responses to drugs.^{10–12} Using CRISPR/Cas9, it is possible to generate a heterogeneous population of cells in which all protein-encoding genes are knocked-out one by one in separate cells by introducing a genome-wide library of guide RNAs (gRNAs) and Cas9 endonuclease. Treatment of this population of cells with a specific drug, for example vincristine, allows resistant cells to be enriched and genes affecting drug sensitivity to be identified by deep sequencing of gRNA cassettes. Using this approach, we have previously uncovered the cellular drug response to rituximab, leading to the identification of the two B-cell receptor (BCR) signalling-related genes *BLNK* and *BTK* as mediators of rituximab-induced death in germinal center B-cell-like (GCB)-subtype DLBCL cell lines.¹³

Using CRISPR-based gene inhibition and activation screening, Palmer et al investigated cross-resistance among the individual R-CHOP components in the DLBCL cell line Pfeiffer and the leukaemia-like cell line K562.¹⁴ Also, CRISPR knockout screening in the acute lymphoblastic leukaemia (ALL) cell line REH was performed to investigate resistance across the seven chemotherapeutics used to treat ALL.¹⁵ This work showed that sensitization of cells towards vincristine was increased by knockout of the gene encoding the small-molecule drug transporter *ABCC1* as well as genes encoding key mitotic factors. Genome-wide screens in DLBCL cell lines have also been used to explore the drug response to CC-122, a cereblon E3 ligase modulator,¹⁶ and tazemetostat, an EZH2-inhibitor.¹⁷ In addition, CRISPR screens were utilized to identify gene knockouts affecting cell survival and proliferation in DLBCL cell lines during normal cell culture.^{18–20}

Here, we use genome-wide CRISPR screening to investigate the cellular response to vincristine in DLBCL cells. We perform gene-set enrichment analysis and use FDRnet to identify subnetworks among sensitizing and resistance-inducing gene knockouts. Based on our screen data and the Bliss analysis model, we identify a small-molecular inhibitor, BTB-1, that works synergistically with vincristine to eradicate cancerous

B-cells. BTB-1 binds specifically to the kinesin-8 motor family member KIF18A and inhibits the motility and chromosome alignment ability of KIF18A.²¹ Moreover, we identify vincristine resistance genes of which knockout interferes with vincristine-induced p53-responses, suggesting an origin of vincristine resistance in the mitotic surveillance pathway. Our findings expand the understanding of the cellular response to vincristine in DLBCL supporting precision oncology.

METHODS

Cell lines

The DLBCL cell lines OCI-Ly7 and SU-DHL-5 were kindly provided by Jose Martinez-Climent (University of Navarra) and obtained from the German Collection of Microorganisms and Cell Cultures (DSMZ), respectively. The cells were cultured in RPMI 1640 supplemented with 10% foetal bovine serum and 1% penicillin/streptomycin. HEK293T cell line was obtained from ATCC. They were cultured in DMEM with 5% foetal bovine serum and 1% penicillin/streptomycin. All cell lines were examined for mycoplasma infection on a regular basis. OCI-Ly7 and SU-DHL-5 were authenticated by DNA barcoding using the sensitive AmpFISTR Identifiler PCR amplification kit (Applied Biosystems). The amplified products were analysed by capillary electrophoresis (Eurofins Medigenomix GmbH, Applied Genetics). The resulting FSA file was analysed using the Osiris software (ncbi.nlm.nih.gov/projects/SNP/osiris), and the identity of the cell lines was established by comparing to DNA barcoding profiles for known cell lines obtained with the same markers and made publicly available at DSMZ.

Plasmids

lentiCas9-Blast (Addgene #52962) and lentiGuide-Puro (Addgene #52963) were kindly provided by Feng Zhang. The Brunello pooled library of gRNAs (Addgene #73178) was kindly provided by David Root. plentiGuide-Puro with MS4A1-targeting gRNA was generated as described by Thomsen et al.¹³

Lentiviral vector production, transduction and titration

For lentiviral vector production, 4×10^6 HEK293T cells were seeded and transfected 24h later with 3 μ g pRSV-REV, 13 μ g pMDIg/pRRE, 3.75 μ g pMD.2G and 13 μ g of the desired lentiviral transgene vector. Transfection was performed using calcium phosphate buffers. Medium was changed 24h after transfection, and 48 hours after transfection, viral supernatants were harvested and filtered through a sterile filter (0.45 μ m). SU-DHL-5 cells were transduced by seeding 4×10^5 cells in a 12-well plate and then adding the viral vector preparation

to a total volume of 1 mL. Titration was performed 96 h after transduction by quantification of the proviral element WPRE in genomic DNA, as described by Ryø et al.²²

Genome-wide CRISPR screening

The plasmid library was amplified as described by Thomsen et al.²³ The screen was performed in a SU-DHL-5/Cas9 clone validated by generating 90% indels ($R^2 = 0.91$) using an *MS4A1*-targeting gRNA. The Brunello library of gRNAs was delivered to the SU-DHL-5/Cas9 clone in duplicates using lentiviral vectors with a transductional titre of 1.3×10^6 IU/mL. To obtain an MOI of 0.5 with 77 441 gRNAs being represented in the screen on average 1000 times, 1.55×10^8 cells were transduced per replicate. Two days after transduction, puromycin selection was initiated and maintained for 1 week. Ten days after transduction, 2×10^8 cells were harvested for genomic DNA extraction, whereas the remaining cells were resuspended in fresh medium with either saline or vincristine added. On day 31 after transduction (3 weeks of drug selection), a minimum of 1×10^8 cells were harvested for genomic DNA extraction using NaCl precipitation, as described by Thomsen et al.²³ PCR amplification of the gRNA cassette and subsequent gel extractions were performed as described by Thomsen et al.²³

Next generation sequencing

Next-generation sequencing was carried out at BGI-Research, Shenzhen. Briefly, PCR amplicons were processed by end repair and ligated to BGISEQ-500 sequencer-compatible adapters. DNA nanoball (DNB)-based sequencing libraries were generated by rolling circle amplifications. The quality and quantity of the sequencing libraries were assessed using Agilent 2100 BioAnalyzer (Agilent Technologies). Finally, the DNB libraries were sequenced with the BGISEQ-500 sequencer (MGI Tech.) with 100 paired-end sequencing with 7.7×10^7 reads per sample replicate on average.

Data analysis of genome-wide CRISPR screening

Cutadapt 2.10 was used to trim the NGS reads to only include the gRNA sequence by detailing the set sequence before and after the gRNA sequence. An error rate of 0.3 and a read length between 17 and 23 were allowed. Bowtie 1.3.0 was used to map the trimmed reads to the Brunello library using the -v 0 -m 1 alignment setting. The gene sets of core essential genes (CEG) and non-essential genes were from Hart et al.²⁴ AUC values of gene sets were calculated using the script Calc_auc_v1.1.py from <https://github.com/mhegde/auc-calculation>. The gene scores were calculated using the algorithm JACKS developed by Allen et al (<https://github.com/felicityallen/JACKS>).²⁵ Gene set enrichment analysis was performed using ShinyGO 0.76.3 (<http://bioinformatics.sdstate.edu/go/>).²⁶ The FDR cut-off was set to 0.05 and the pathway size set to minimum 2 and

maximum 2000. The 267 and 166 genes with the highest and lowest JACKS score, respectively, and a *p*-value below 0.01, common for both high- and low dose vincristine samples, were analysed. To identify the most significant subnetworks, the algorithm FDRnet developed by Yang et al.²⁷ (<https://github.com/yangle293/FDRnet>) was used with the STRING protein-protein interaction network version 11.5 and FDR values calculated using Benjamini-Hochberg's method from *p*-values calculated using JACKS gene scores. The STRING protein-protein interaction network was filtered to only include interactions with high confidence. This was done by only including interactions with a STRING-reported 'combined score' above 500 except for genes with less than five interactions where all interactions were included to ensure that all genes were represented. This resulted in a database of 384 290 protein-protein interactions. The software tool Cytoscape version 3.8.2 with the packages DyNet and clusterMaker was used to visualize the identified subnetworks. Plots were generated in R using the packages ggplot2, ggrepel and ggprism and modified in Adobe Illustrator version 2020.

Generation of gene knockout in cells by nucleofection, indel analysis and deep sequencing

For nucleofection, 3.2 µg chemically modified (2'-O-methyl at 3' first and last bases, 3' phosphorothioate bonds between first 3 and last 2 bases) gRNA (Synthego) and 6 µg Cas9 protein (Alt-R S.p. Cas9 Nuclease V3, Integrated DNA Technologies) were incubated at 25°C for 15 min before mixing with 6×10^5 cells, which were rinsed and suspended in 20 µL OptiMEM. The cells were nucleofected using a 4D-nucleofector device (Lonza) in 20-µL Nucleocuvette strips (Lonza). Cells were nucleofected using the program CM-125 or CM-130 set to P3 buffer. Following nucleofection, the cells were seeded in 100 µL pre-heated medium in a 96-well plate. The following day, the cells were transferred to a 48-well plate and 100 µL medium was added before the cells were expanded. Indel analysis was performed as described by Ryø et al.²² using ICE software tool (Synthego, <https://ice.synthego.com/>). Deep sequencing of cut-site was done by Eurofins using INVIEW CRISPR CHECK and 2nd PCR Protocol. CRISPResso2 was used to analyse the raw NGS reads for genome editing (<http://crispresso2.pinellolab.org/>).²⁸

Flow cytometry-based assays

Prior to the seeding of cells, the proliferation rate was aligned by passing the cells every second day and seeding them at the same density at either 4×10^5 or 5×10^5 cells/mL for SU-DHL-5 and OCI-Ly7, respectively. This was done for a minimum of 3 passages before the assay initiation. For the assays, 7.2×10^4 SU-DHL-5 or 9.0×10^4 OCI-Ly7 cells were seeded in a 96-well plate in 175 µL medium in a random set-up to avoid bias from the flow cytometer running order. In drug assays, drug,

DMSO, or saline was added in 5 μ L. After 48–60 h, the cells were passaged by removing and replenishing 120 or 100 μ L medium for SU-DHL-5 or OCI-Ly7 cells, respectively. In drug assays comparing gene knockouts to wildtype, vincristine or saline was added as well when passaging the cells, whereas only medium was replenished in drug synergy assays. After 110–120 h, the samples were mixed and 97 μ L cell suspension was transferred to a V-bottom 96-well plate with 2.5 μ L 50 μ g/mL propidium iodide. The number of live and dead cells in 30 μ L was counted using a NovoCyte 2100YB Flow Cytometer (Agilent Technologies). Vincristine sulfate (Merck) was dissolved and diluted in saline. BTB-1 (Axon Medchem) was dissolved in DMSO and diluted in saline. For intracellular staining of p53, cells from 3 wells were pooled and washed in 1% BSA (bovine serum albumin) in PBS and then stained with Fixable Viability Dye eFluor 780 (Invitrogen) as viability marker for 15 min at 4°C. Cells were washed again before using ice-cold methanol for fixation and permeabilization for 2 min, and then washed and stained with PE-conjugated p53 antibody (Clone DO-7, BioLegend, Cat. 645805) 1:100 in 0.1% Triton X-100 0.5% BSA in PBS at room temperature for 30 min prior to a wash in 1% BSA in PBS, and run on NovoCyte Quanteon 4025 Flow Cytometer (Agilent Technologies). For the cell cycle assay, cells from 3 wells were pooled and the 488 EdU Click Proliferation Kit (BD Biosciences) was used using Fixable Viability Dye eFluor 780 (Invitrogen) as viability marker and propidium iodide as DNA staining without adjusting dye/cell ratio. Ice-cold methanol was used for fixation and permeabilization. For the apoptosis assay, the CellEvent Caspase-3/7 Green Detection kit (Invitrogen) was used with propidium iodide as a viability marker. Nutlin-3 (Merck) was dissolved in DMSO and diluted in saline.

Western blotting

For Western blotting, 1×10^6 cells were washed in PBS and lysed in RIPA Lysis and Extraction buffer (ThermoFisher Scientific, Cat. 89901) supplemented with 10 mM NaF and 1x complete protease inhibitor cocktail (Roche). Then, XT Sample Buffer, 4x (Biorad, Cat. 161-0791) and XT Reduction Detergent 20x (Biorad, Cat. 161-0792) were added to the samples, and the samples were boiled for 5 min before being loaded on the gel (4%–15% Criterion TGX Precast Midi Protein Gel, Bio-Rad). Proteins were separated by SDS-PAGE and blotted into a polyvinylidene fluoride membrane. Membranes were divided in two by cutting at the 100 kDa mark. Membranes were blocked in 5% skim milk in TBS supplemented with 0.005% Tween-20 (Sigma-Aldrich). The bottom and top parts of the membrane were then incubated overnight at 4°C with primary p53 antibody (2 μ g/mL, 1:250) (Clone DO-1, BD Biosciences, Cat. 554293) and primary vinculin antibody (1:10000) (Clone hVIN-1, Sigma Aldrich Cat. V9131), respectively. The membranes were then washed in TBS supplemented with 0.005% Tween-20 (Sigma-Aldrich) and incubated with horseradish peroxidase (HPR)-conjugated secondary antibody and visualized by

chemiluminescence using a HPR substrate (Bio-Rad, Cat. 170-5061). Quantification was performed using ImageJ.

RNA extraction and qPCR of gene expression

For RNA extraction, 1×10^6 cells were lysed with 0.5 mL TRI Reagent™ Solution (Fischer Scientific, Cat. AM9738), followed by the addition of 0.1 mL Chloroform. After mixing and 3 min of incubation at room temperature, the samples were centrifuged at 17000 *g* for 15 min at 4°C. Hereafter, 300 μ L of the aqueous phase was mixed with 375 μ L ethanol and loaded onto a column from the hiPure miRNA purification kit (Roche, Cat. 5080576001). The samples were washed and eluted according to the manufacturer's instructions. Then, 800 ng RNA was treated with DNase I (Thermo Fisher Scientific, Cat. EN0521) in a total volume of 10 μ L, for 30 min at 37°C. Hereafter, the DNase was inactivated by the addition of 1 μ L 50 mM EDTA followed by incubation at 65°C for 10 min. For cDNA synthesis, 500 ng DNase-treated RNA was used in a 10 μ L reaction using Maxima H Minus cDNA Synthesis Master Mix (Thermo Fisher Scientific, Cat. M1662). For qPCR, 4.8 μ L 10-fold diluted cDNA was used in a 10 μ L reaction with 500 nM forward and reverse primer, using RealQ Plus 2x Master Mix Green (Ampliquon, Cat. A323402). The primers were designed to span an exon-exon junction to avoid contamination from genomic DNA. The qPCR was run on a Lightcycler 480 II (Roche) in technical triplicates. The relative expression levels were determined using a standard delta–delta CT calculation normalized to GAPDH.

Statistical analysis

One-way ANOVA was performed in the software program GraphPad Prism version 9. If a *p*-value below 0.05 was calculated, then Dunnett's multiple comparison test was used to compare the mean of the samples with the corresponding control sample.

Data sharing statement

NGS fastq files from genome-wide CRISPR screening are available from the corresponding author upon request. Read count table and JACKS gene score table for CRISPR screening data can be found in supplementary tables.

RESULTS

Uncovering genes affecting the response to vincristine by genome-wide CRISPR screening in SU-DHL-5 cells

To identify genes affecting the response to vincristine in DLBCL cells, we performed genome-wide CRISPR screening

in the GCB-subtype SU-DHL-5 cell line (Cas9-expressing clone), which is more sensitive to vincristine than other DLBCL cell lines.²⁹ We used the Brunello library developed by Doench et al targeting 19 114 genes with 4 gRNAs per gene on average (Figure 1A).³⁰ After transduction and a selection for gRNA-containing cells only, we challenged the cells with vincristine at a low (1.3 ng/mL) and high (1.7 ng/mL) concentration (Table 1) in two independent replicates for 3 weeks before harvesting cell pellets for NGS sequencing.

The coverage of each gRNA in each sample was on average 450 and 323 at minimum. The plasmid sample had a low Gini index³² of 0.062 indicating that the gRNAs were close to equally distributed, and less than 0.1% of the gRNAs were unaccounted for (Figure 1B). To ensure high screen quality, we used the core essential and non-essential gene sets established by Hart et al.²⁴ and made empirical cumulative distribution functions (ECDF) of gRNA rankings (Figure 1C). All samples showed high area under curve (AUC) values of the ECDF near or above 0.90 for the CEG (Figure 1D). This demonstrated a high efficiency in generating gene knockout and selecting cells based on the phenotypic consequence across all samples.

We compiled the gRNA read counts into gene scores using the JACKS algorithm, which takes varying gRNA efficiency into account when assigning gene scores.²⁵ Saline-treated replicates were used as baseline against the two replicates for each vincristine concentration, resulting in JACKS scores for high and low vincristine concentrations. High JACKS gene scores indicated that genes with CRISPR/Cas9-induced loss-of-function made the cells more resistant towards vincristine, whereas low JACKS scores indicated that the cells became sensitive to the drug. Genes with CRISPR/Cas9-induced loss-of-function will from here on be referred to as LOF genes. The JACKS scores showed high correlation when plotting the high-dose scores against the low-dose scores, demonstrating that the same LOF genes had the highest impact across both drug concentrations (Figure 1E). Notably, sensitizing LOF genes had a higher impact in the low-dose condition, whereas resistance-mediating LOF genes had a higher impact in the high-dose condition. The *ABCC1* (*MRP1*) gene encoding an ABC transporter known for mediating multi-drug resistance was one of the genes with the lowest JACKS score.³³ This served as an initial validating proof that the

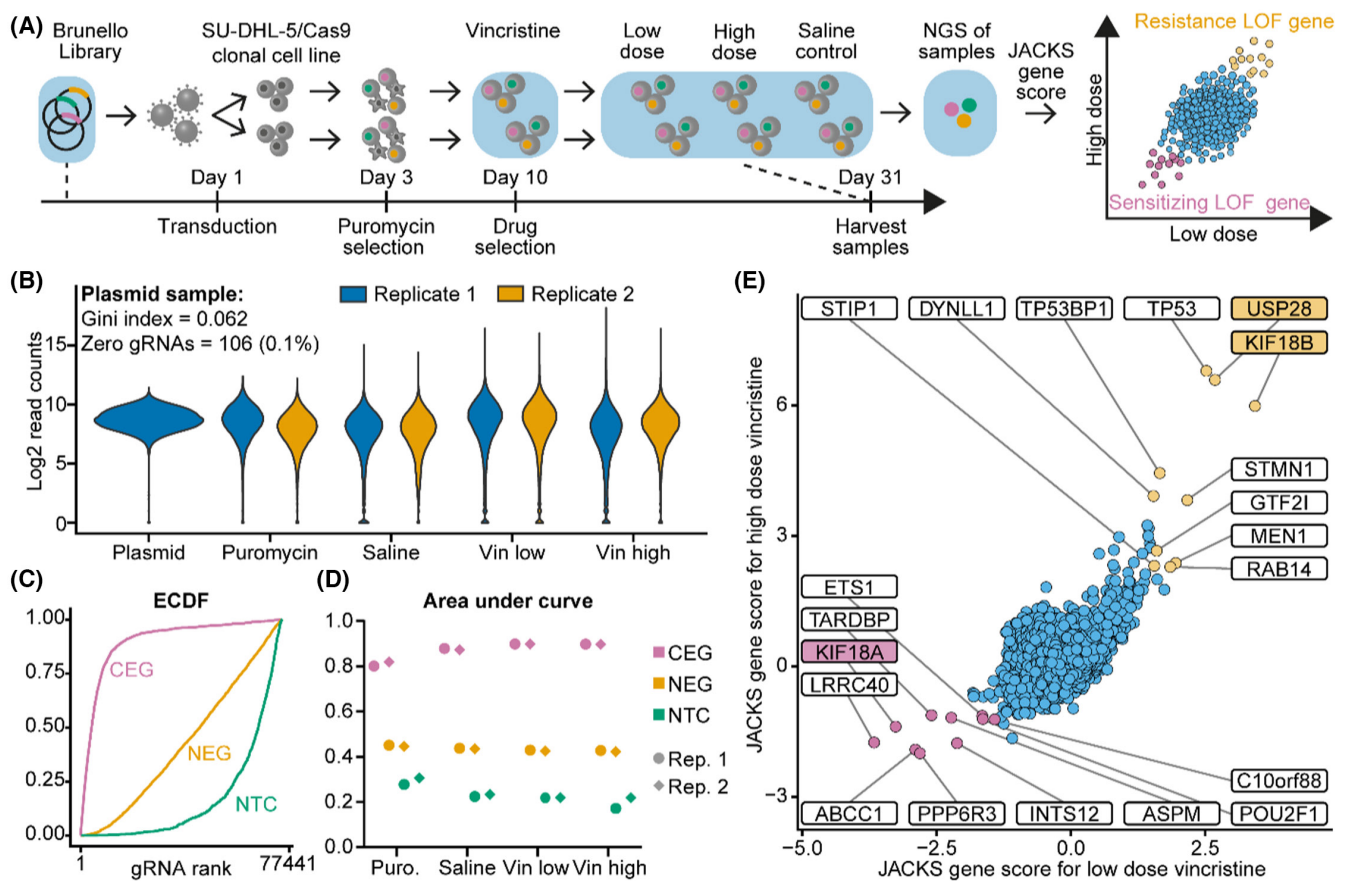


FIGURE 1 Genome-wide CRISPR screening using vincristine as selective pressure. (A) The genome-wide CRISPR screening process and how the samples indicated with blue background were generated. (B) Distribution of log₂-normalized read counts of gRNA sequences in NGS data. (C) Empirical cumulative distribution functions (ECDF) plotted for gRNAs targeting core essential genes (CEG), non-essential genes (NEG), and non-targeting controls (NTC). Optimally, gRNAs targeting CEG should have a low rank, due to successful gene knockout causing cell death. (D) Area under the curve (AUC) values plotted for ECDFs across the three gene sets and all samples. (E) JACKS gene scores for the low- and high-dose vincristine samples plotted against each other.

TABLE 1 Vincristine dose response values from Falgreen et al.³¹

Cell line	GI50 (ng/mL)	TGI (ng/mL)	LC50 (ng/mL)	Cell seeding (cells/mL)
SU-DHL-5	0.71	1.00	1.70	2.5 × 10 ⁵
OCI-Ly7	2.55	2.90	3.39	2.5 × 10 ⁵

Abbreviations: GI50, 50% cell growth inhibition; LC50, 50% cell death; TGI: total growth inhibition.

screening approach uncovered genes with a high impact on the cellular vincristine response.

Significant pathways, subnetworks and protein complexes in the cellular response to vincristine

To identify more general tendencies at the pathway level, we used ShinyGO to perform and visualize gene-set enrichment analysis using Gene Ontology (GO) and Reactome databases.²⁶ For the 166 genes with a low JACKS score and a *p*-value below 0.01 for both the high- and low-dose samples, gene sets related to microtubule depolymerization, mitotic spindle organization, INO80 complex, and DNA damage recognition in Global-Genome Nucleotide Excision Repair (GG-NER) were among the enriched gene sets (Figure S1A–C). For the 267 genes with a high JACKS score and a *p*-value below 0.01 for both the high- and low-dose samples, gene sets related to negative regulation of mTOR signalling, GATOR1-complex, CD40 receptor complex and Rab GTPases regulation of trafficking were among the enriched gene sets (Figure S2A–C).

The algorithm FDRnet was developed by Yang and colleagues to identify subnetworks of cancer drivers in genomic datasets with high gene scores and high connectivity within larger networks.²⁷ Here, we used FDRnet to identify subnetworks and protein complexes with significant influence on the vincristine response as suggested by our screen data (Figure 2A). We used JACKS-derived FDR values and the STRING protein–protein interaction network but only included high-confidence interactions with direct evidence of physical protein–protein interactions. Among the most sensitizing LOF genes, we identified subnetworks related to mitotic spindle organization, the cytoplasmic dynein complex responsible for trafficking along microtubules, and the INO80 complex, an ATP-dependent chromatin remodeler (Figure 2B).³⁴ The subnetworks identified for resistance-mediating LOF genes included BCR signalling, tumour necrosis factor receptor (TNFR) signalling entailing CD40 receptor signalling, membrane trafficking represented by Rab GTPases and the GATOR1 and TSC1/2 complex, which both negatively regulate mTOR signalling (Figure 2C). Except for subnetworks related to GG-NER, the FDRnet approach identified subnetworks related to the same biological processes as the most enriched gene-sets in the gene-set enrichment analysis. In addition, *TP53* was

discovered to be a key gene as a central connection for many of the identified subnetworks.

We have previously shown that knockout of genes related to BCR signalling, including *BLNK* and *BTK*, rendered the GCB-subtype DLBCL cell lines OCI-Ly7 and SU-DHL-5 more tolerant towards rituximab.¹³ Notably, median-normalized read counts showed that gRNAs targeting *BLNK* and *BTK* were enriched in the saline-treated sample compared to the baseline in the plasmid sample. This implies that knockout of these genes confers increased survival signalling and proliferation during normal cell culture (Figure S3A,B). To identify the subnetworks that impacted the survival and proliferation rate during normal cell culture, we colour-coded the genes according to their JACKS scores for saline-treated samples, where the initial plasmid sample was used as baseline (Figure S4A–C). Besides BCR signalling, genes related to TNFR signalling and the GATOR1 complex and the genes *PTEN* and *NFKBIA* also had high JACKS scores for the saline-treated samples. Notably, all these subnetworks and genes are involved in NF-κB and PI3K-AKT-mTOR signalling, which regulates survival signalling, proliferation and stress responses.^{35,36} This indicates that increased tolerance to vincristine can be induced by LOF genes leading to more proliferation and survival signalling in general.

In summary, a subset of LOF genes related to mitotic spindle organization sensitize the cells to vincristine with little impact during normal cell culture, and *TP53* is a central component connecting the FDRnet-discovered subnetworks with LOF genes that increase the tolerance to vincristine.

KIF18A-inhibitor BTB-1 acts synergistically with vincristine in eradicating DLBCL cells

Our screen uncovered genes related to mitotic spindle organization to be essential for the DLBCL cells to survive vincristine treatment. Median-normalized read counts for gRNAs targeting *KIF18A*, a kinesin-8 motor family member involved in chromosome alignment during mitosis,³⁷ showed that gene knockout sensitized the DLBCL cells to vincristine without affecting the saline-treated samples (Figure 3A). We used the KIF18A-inhibitor BTB-1²¹ to test if the screening results could be used to identify targets for small-molecule inhibitors that act synergistically with vincristine in killing DLBCL cells.

Treating SU-DHL-5 cells with either vincristine (dosages ranging from 0 to 2.0 ng/mL) or BTB-1 (dosages from 0 to 20 μg/mL) one at a time did not result in cell death. However, the combination of the two drugs led to extensive cell death with the highest drug concentrations resulting in less than 6% viable cells (Figure 3B). Notably, in these drug assays, the cell density at seeding were higher than in drug assays performed in Table 1, resulting in higher doses needed to reach LC50. A similar pattern was observed in OCI-Ly7 cells, in which combinations of vincristine

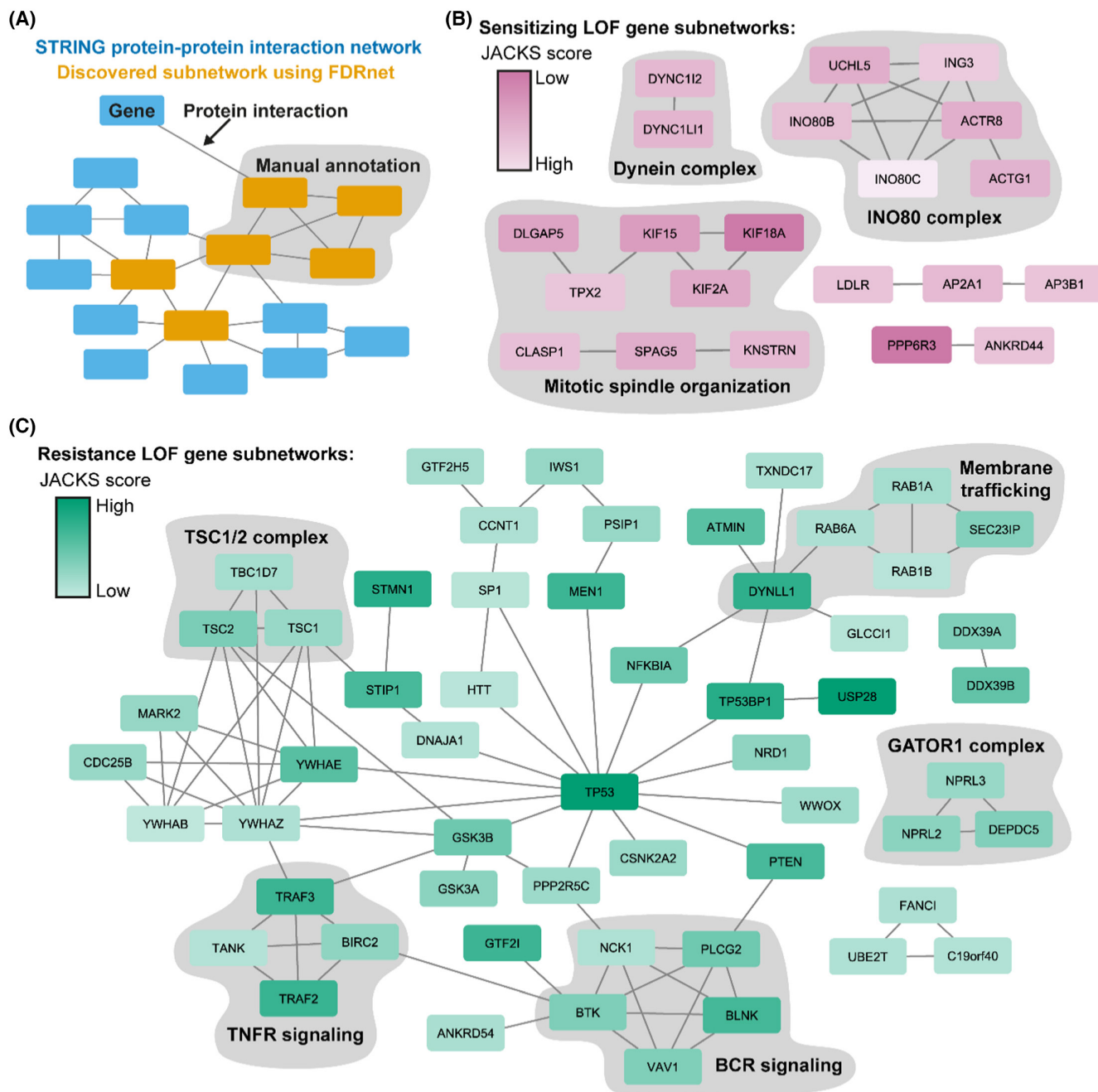


FIGURE 2 Subnetworks of important genes in the response to vincristine identified using FDRnet. (A) The STRING protein-protein interaction network in blue with an FDRnet-discovered subnetwork in orange. The grey clouds indicate manually annotated descriptions of the unifying biological process or protein complex. (B, C) The FDRnet-identified subnetworks among the most sensitizing (B) and resistance-inducing (C) LOF genes.

(0–3.2 ng/mL) and BTB-1 (0–20 µg/mL) led to complete cell death, whereas the drugs individually had no measurable effect (Figure 3C). Robust synergistic effects of using BTB-1 together with vincristine was confirmed using the Bliss Independence Model¹⁴ (Figure 3D) on cell counts of viable cells for SU-DHL-5 (Figure 3E) and OCI-Ly7 (Figure 3F). Together, our findings identify a potential new DLBCL drug target and demonstrate the capacity of genome-wide CRISPR screening to uncover synergistic drug interactions exemplified by the substantial synergistic effect of BTB-1 on vincristine-induced cell death.

KIF18B and *USP28* knockout increases tolerance towards vincristine

Together with *TP53*, the genes *KIF18B* and *USP28* had significantly higher JACKS scores than all other genes, and gRNAs targeting these genes only showed strong enrichment in samples treated with vincristine, but not in saline-treated samples (Figure 4A,B). *KIF18B* encodes, like *KIF18A*, a kinesin-8 motor family member involved in mitotic spindle organization by regulating astral microtubules,³⁸ whereas *USP28* encodes a de-ubiquitinase regulating many cancer-related

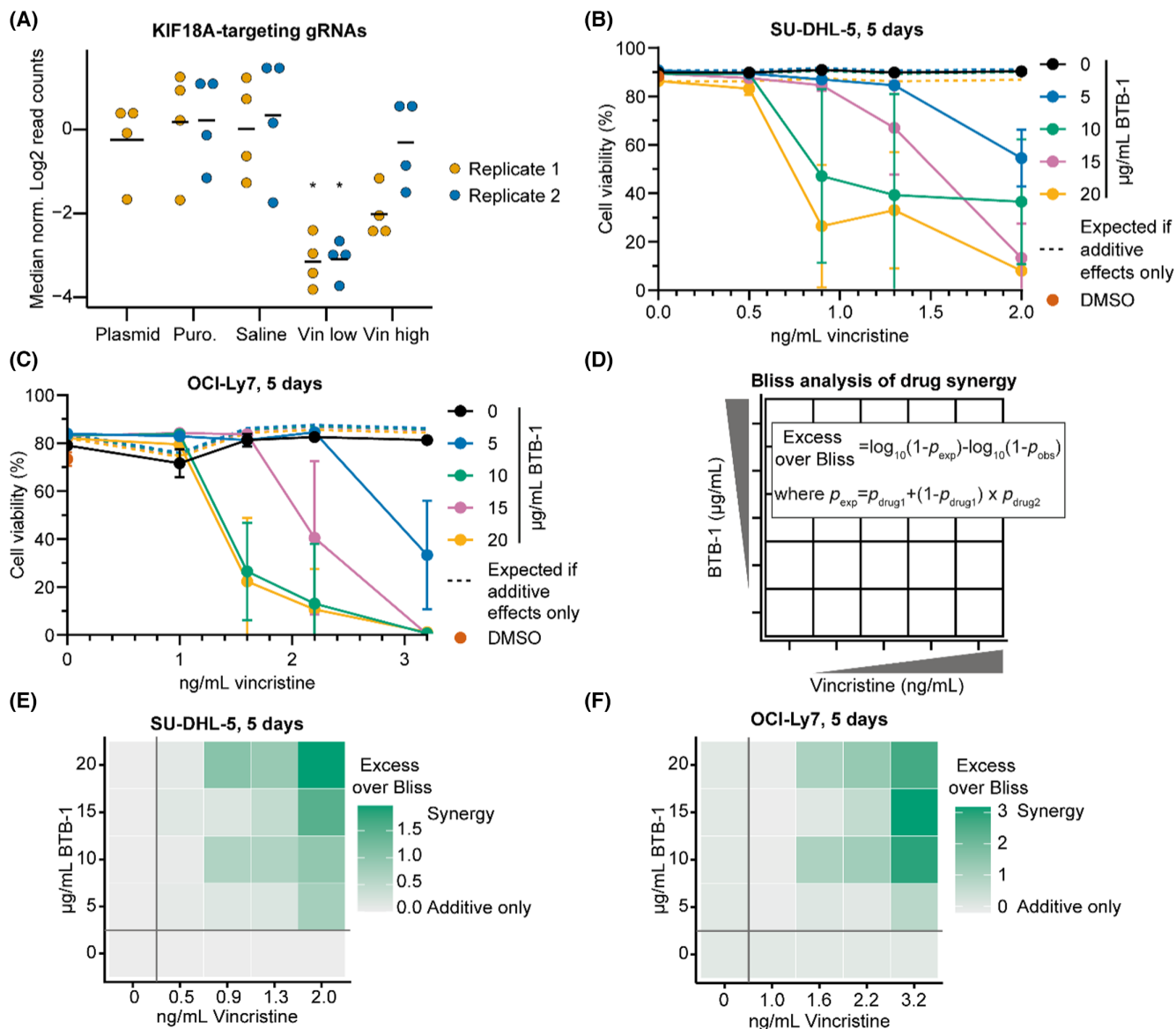


FIGURE 3 The KIF18A-inhibitor BTB-1 combined with vincristine shows synergistic effect in eradicating DLBCL cells. (A) Median normalized log₂ read counts of gRNAs targeting *KIF18A* in the genome-wide CRISPR screening. (B, C) Drug assays in SU-DHL-5 (B) and OCI-Ly7 (C) cells showing the synergistic effect of vincristine and BTB-1. The dotted lines indicate theoretically calculated values showing the expected effect if the individual drug effect combined was only additive. These values were calculated using the Bliss analysis model. Drug assays were performed by counting live and dead cells after propidium iodide viability staining on a flow cytometer. (D) The Bliss analysis used to model the individual drug effects to test whether the drug interaction effect is synergistic or additive. Here, p_x denotes the proportion of cells at the particular dose of the particular drug(s) compared to saline-treated cells. p_{drug1} , p_{drug2} and p_{obs} is the proportion for vincristine, BTB-1, and combined, respectively. (E, F) The Bliss analysis for cell counts of live cells for SU-DHL-5 (E) and OCI-Ly7 (F) cells. Drug assays in (B, C) and (E, F) show data from an individual experiment with four replicates per sample.

pathways.³⁹ To generate SU-DHL-5 and OCI-Ly7 cell lines with knockout of either *KIF18B* or *USP28*, we nucleofected cells separately with two gRNAs for each gene, generating robust indel rates around 90% and at minimum 72% after 8 days. To ensure the stability of the established knockout populations, we confirmed comparable indel rates and indel patterns 25 days or more after the initial measurement (Figure 4C and Figure S5A,B). Cells treated with two control gRNAs targeting safe-harbour loci were also included (Figure S5B).

In addition, to further increase the knockout rate, cell populations generated using the first gRNAs were nucleofected with the second gRNAs targeting the same gene. Deep sequencing of the gRNA-targeted *KIF18B* and *USP28* loci verified extensive gene disruption (Figure 4D). Hence, less than 3% of the sequenced alleles mapped to wildtype sequence in SU-DHL-5 and OCI-Ly7 cells, and more than 83% of the sequenced alleles had frameshifts or indels spanning 15 or more nucleotides. For both loci, the two gRNAs recognizing closely located binding sites induced large deletions

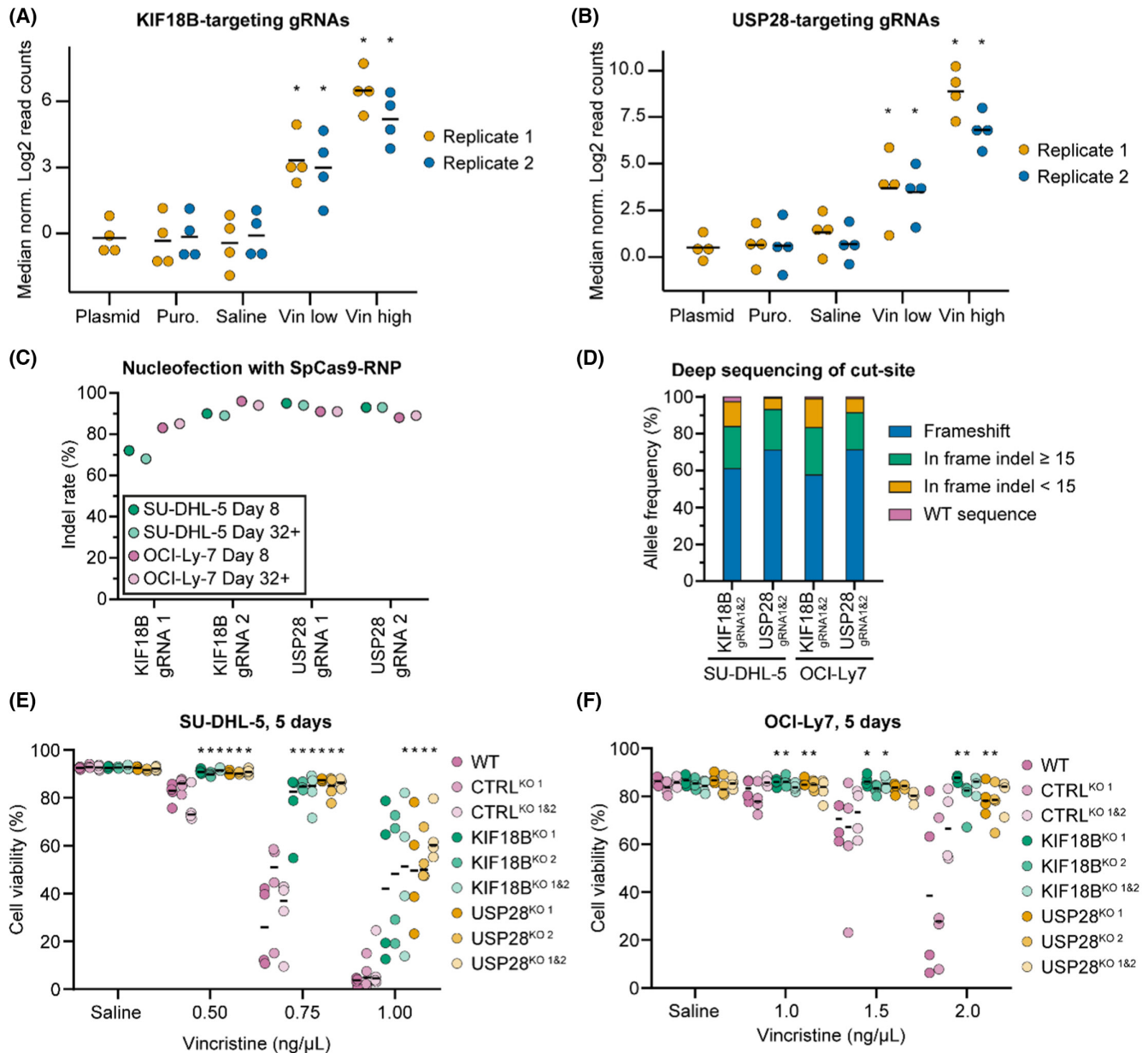


FIGURE 4 *KIF18B* and *USP28* knockout induces resistance to vincristine. (A, B) Median normalized log₂ read counts of gRNAs targeting *KIF18B* (A) and *USP28* (B) in the genome-wide CRISPR screening. The plasmid sample was used as control for performing Dunnett's multiple comparison test. (C) Indel rates measured after Cas9-induced gene knockout using Sanger sequencing at day 8 or more than 32 days after nucleofection. (D) Allele frequencies of indels in double knockout generated cell lines by deep sequencing (>119 000 reads) of the cut-site. (E, F) Drug assays in SU-DHL-5 (E) and OCI-Ly7 (F) generated gene knockout cell lines. Drug assays were performed by counting live and dead cells after propidium iodide viability staining on a flow cytometer. Data for an individual experiment with four replicates per sample. For samples treated with the same dose of vincristine, the samples treated with either 1 or 2 gRNAs were compared to the control sample treated with 1 or 2 gRNAs, respectively, when performing Dunnett's multiple comparison test.

above 70bp in more than 15% of the sequenced alleles (Figure S5C,D). The high frequency of frameshift mutations and large deletions led to reduced mRNA expression due to nonsense-mediated mRNA decay for the *USP28* transcript, but not for *KIF18B* (Figure S5E,F). For *KIF18B*, however, the gRNAs were designed to target exon 1 encoding the essential motor domain of KIF18B protein responsible for binding microtubules.

In both SU-DHL-5 and OCI-Ly7 cells, knockout of either *KIF18B* or *USP28* strongly increased the tolerance towards vincristine. For SU-DHL-5 cells treated with 0.75 ng/mL vincristine twice during 5 days, the average viability of naïve cells and the control cells generated using irrelevant gRNAs was below 44%, whereas the *KIF18B*- and *USP28*-deficient cells were more resistant with viabilities above 76% (Figure 4E). Notably, in these drug assays vincristine

was replenished after 48–60 h. For OCI-Ly7 cells cultured in 2.0 ng/mL vincristine, the average viability for naïve and control gRNA-generated cells was between 34% and 68%, whereas the *KIF18B*- and *USP28*-deficient cells showed viabilities comparable to the saline condition above 77% (Figure 4F). In summary, these data demonstrate that lack of either *KIF18B* or *USP28* renders GCB-subtype DLBCL cells more resistant to vincristine.

KIF18B and USP28 mediate accumulation of activated p53 during vincristine treatment

The FDRnet analysis revealed *TP53* as a central gene connecting most subnetworks found among resistance-mediating LOF genes including a connection to *USP28* through *TP53BP1*. In fact, upon prolonged mitosis, *USP28* has been shown to de-ubiquitinate and, thus, stabilize p53 through binding the scaffold protein 53BP1 (encoded by *TP53BP1*) leading to cell cycle arrest and apoptosis.^{8,40} We speculated that resistance to vincristine induced by *KIF18B* and *USP28* deficiency could be explained by their influence on restricting this p53 response.

To study the role of p53, we first examined the effect of vincristine on p53 expression. Western blotting showed an increased level of p53 upon vincristine treatment in SU-DHL-5 cells, whereas the effect on p53 was less pronounced in *KIF18B* and *USP28* knockout cells (Figure 5A,B). OCI-Ly7 cells showed a constitutively high level of p53 protein, which did not increase further upon vincristine treatment (Figure 5A,B). Notably, *TP53* in OCI-Ly7 cells carries a variant causing a glycine to aspartic acid change in the DNA binding domain of p53 (p.G245D), which destabilizes the protein and increases the amount of misfolded, non-functional protein.⁴¹

Flow cytometry-based intracellular staining of p53 showed that knockout of *KIF18B* or *USP28* in SU-DHL-5 cells drastically decreased vincristine-induced accumulation of p53 (Figure 5C). The single-cell output revealed that only some cells showed induction of p53, reflecting a dynamic nature of p53 expression (flow plots available in Appendix S2).⁴² p53 is negatively regulated by MDM2 by ubiquitination leading to degradation.⁴³ We used nutlin-3, a small molecule inhibitor of MDM2, to inhibit MDM2 function and found in SU-DHL-5 cells that the ability of vincristine to induce p53 expression was restored in *KIF18B* and *USP28* knockout cells exposed to nutlin-3 (Figure 5C). For OCI-Ly7, a constitutively high level of p53 protein was seen across all conditions with a median p53 level that was on average 10-fold higher than the level in SU-DHL-5 (Figure 5D). For both cell lines, noteworthy changes of *TP53*, *KIF18B*, *USP28* or *TP53BP1* mRNA levels were not observed after 24 or 48 h of vincristine treatment (Figure 5E,F), suggesting that vincristine treatment did not support upregulation of p53 at the transcriptional level. Collectively, our findings suggest that *KIF18B* and *USP28* are crucial for the accumulation of p53 upon vincristine treatment in *TP53* wildtype cells.

KIF18B and USP28 mediate induction of cell cycle arrest and apoptosis upon vincristine treatment

We speculated that reduced p53 accumulation in *KIF18B*- and *USP28*-deficient cells would lead to less p21 activation and thus, less vincristine-induced cell cycle arrest and apoptosis. Cell cycle analysis in SU-DHL-5 cells showed that vincristine treatment in control samples (naïve cells and cells treated with irrelevant gRNAs) reduced the percentage of cells actively replicating DNA in S-phase from 64% in saline-treated samples to 19% (Figure 6A). For OCI-Ly7, vincristine treatment reduced the percentage of cells in S-phase from 64% in saline-treated samples to 40% (Figure 6B). For both SU-DHL-5 and OCI-Ly7, the knockout of *KIF18B* led to 10% more cells in S-phase compared to control samples. Likewise, knockout of *USP28* increased the number of cells in S-phase in SU-DHL-5 with 19%, but did not have a similar effect in OCI-Ly7. In both SU-DHL-5 and OCI-Ly7, treatment with nutlin-3 increased the level of p53 (Figure 5C,D) and reverted the effect of *KIF18B* and *USP28* knockout (Figure 6A,B). The effect of nutlin-3 seemed to be more pronounced for the samples given vincristine compared to saline, suggesting that cell cycle arrest was not only affected by the p53 level, but also by a vincristine-driven activation of p53. Notably, vincristine treatment has been shown to induce accumulation and extensive phosphorylation of p53 in epithelial tumour cells.⁴⁴

Next, we examined the effect of *KIF18B* and *USP28* knockouts on vincristine-directed induction of apoptosis by measuring the proteolytic activity of caspase-3 and caspase-7. In SU-DHL-5 control samples, vincristine treatment induced 42% pre-apoptotic cells, which was reduced to 35% and 25% for *KIF18B* and *USP28* knockout samples, respectively (Figure 6C). In OCI-Ly7 control samples, vincristine treatment induced 42% pre-apoptotic cells, which was reduced to 29% for *KIF18B* knockout, whereas there was no change for *USP28* knockout (Figure 6D). By treating the cells with nutlin-3, the reduction in apoptosis in the *KIF18B* and *USP28* knockout samples was reverted. This effect was only seen for samples treated with vincristine, whereas nutlin-3 had no effect on apoptosis in saline-treated samples, supporting the suggestion that vincristine resulted in activation of p53 to induce apoptosis. Collectively, these results demonstrate that *KIF18B* and *USP28* are mediators of vincristine-induced cell cycle arrest and apoptosis.

DISCUSSION

The heterogeneity of DLBCL makes it challenging to predict the best treatment strategy, especially for high-risk patients.² To address this issue, clinical trials have investigated ex vivo platforms for pharmacological testing as an approach to identifying personalized treatment options.^{45,46} We show that genome-wide CRISPR screening using a drug as selective pressure can be used to identify drug targets that result

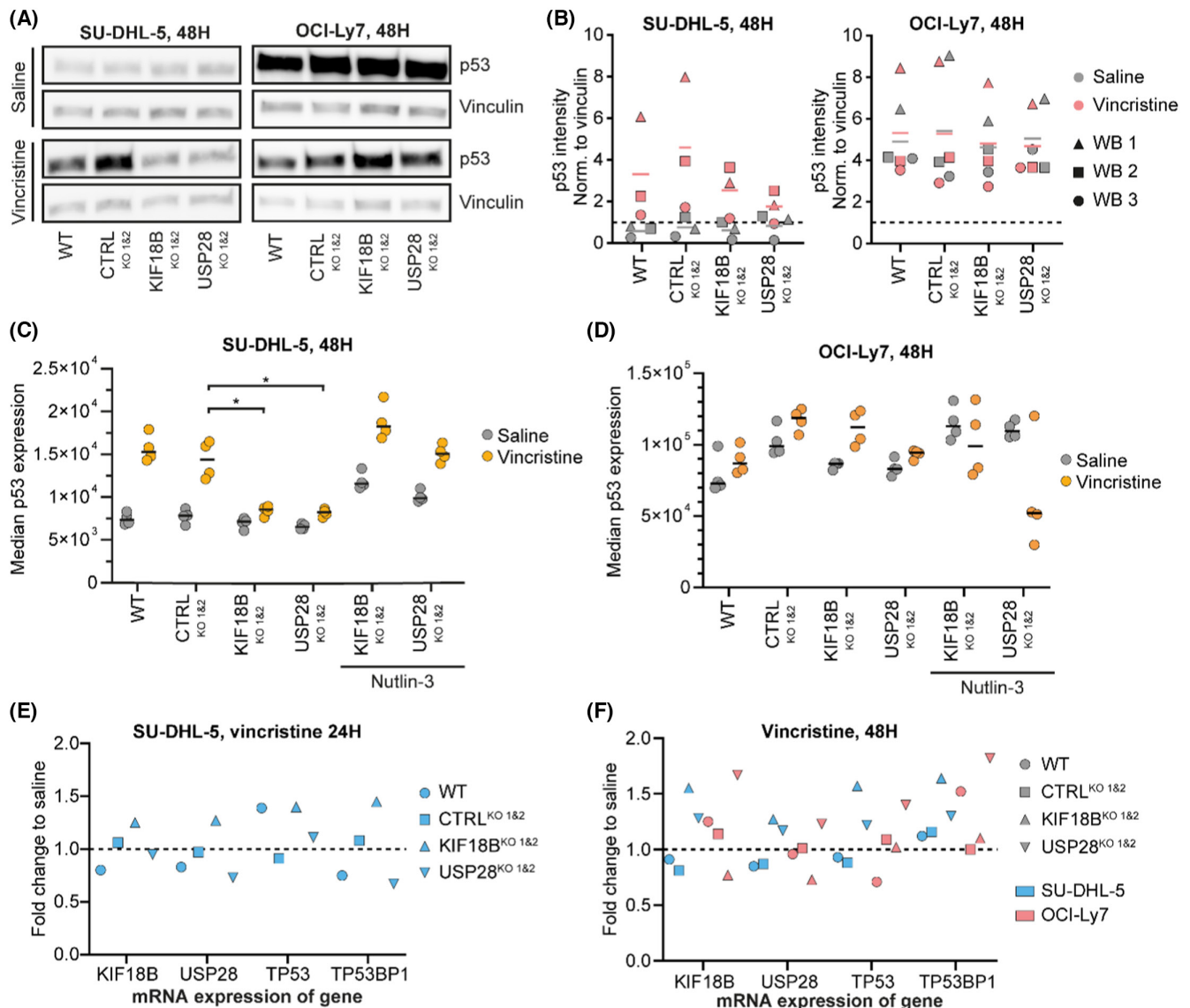


FIGURE 5 *KIF18B* and *USP28* knockout affects vincristine-induced p53 accumulation. (A) Representative Western blot of p53 and vinculin protein comparing vincristine to saline treatment after 48 h. (B) Quantification of 3 Western blots performed using ImageJ. Quantification shows p53 intensity normalized to vinculin for each sample. The uncropped Western blots used for quantification are shown in Appendix S2. WB: Western blot (C, D) Median fluorescence intensity of intracellular staining of p53 protein determined by flow cytometry for SU-DHL-5 (C) and OCI-Ly7 (D) cells after 48 h. Data for an individual experiment with 4 replicates per sample. The CTRL^{KO 1&2} sample was used as control for performing Dunnett's multiple comparison test for samples treated with vincristine. (E) mRNA expression after 24 h of vincristine treatment in SU-DHL-5 cells measured by qPCR. (F) mRNA expression after 48 h of vincristine treatment in SU-DHL-5 and OCI-Ly7 cells measured by qPCR. Data for an individual experiment with 1 replicate per sample run in technical triplicates.

in substantial synergistic effects. CRISPR screening excels as a high-throughput method that enables simultaneous testing of thousands of drug targets using only a fraction of the cells required for testing single drugs one or two at a time. Our CRISPR screening approach identified genes related to mitotic spindle organization as targets for sensitizing cells to vincristine treatment including *KIF15* and *KIF2A* (Figure 7A).^{47,48} This was verified for the kinesin *KIF18A* using the inhibitor BTB-1. *KIF18A* mediates chromosome alignment during metaphase using its plus-end-directed motor on kinetochore microtubules and by regulating spindle length.³⁷ Loss of *KIF18A* has been shown to result in high

chromosome instability in aneuploid cells showing particular dependence on *KIF18A* compared to near-diploid cancer cells during SAC inhibition treatment such as vincristine, which could explain the observed synergistic interaction between vincristine and BTB-1.⁴⁹

Our screening approach also identified genes related to BCR and TNFR signalling, which upon knockout increased the tolerance to vincristine and improved the survival and proliferation rate during normal cell culture (Figure 7A). BCR-signalling through *BLNK*, *BTK* and *PLCG2* follows the canonical NF- κ B pathway causing the release and translocation of p65 (*RELA*), C-Rel (*REL*) and

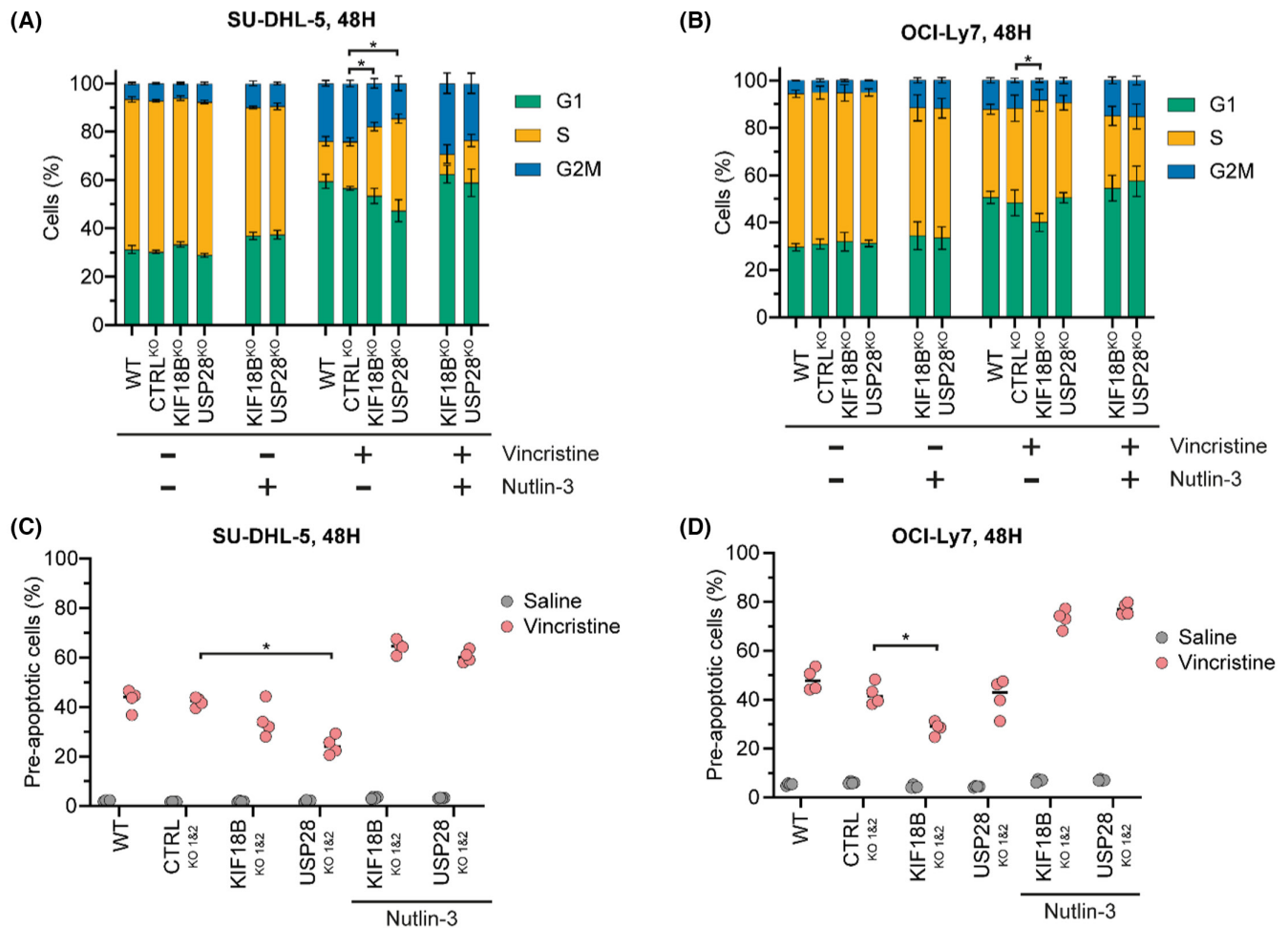


FIGURE 6 *KIF18B* and *USP28* knockout affects vincristine-induced cell cycle arrest and apoptosis. (A, B) Cell cycle analysis for SU-DHL-5 (A) and OCI-Ly7 (B) cells showing the percentage of cells in either G1-, S- or G2/M-phase measured by incorporation of the nucleoside-analogue EdU and DNA binding of propidium iodide by flow cytometry. (C, D) Percentage of pre-apoptotic cells in SU-DHL-5 (C) and OCI-Ly7 (D) measured by proteolytic activity of caspase-3 and caspase-7 in cleaving a fluorogenic substrate in live cells by flow cytometry. For SU-DHL-5, 2 ng/mL vincristine and 1.0 µg/mL nutlin-3 were used and for OCI-Ly7, 3.0 ng/mL vincristine and 2.5 µg/mL nutlin-3 were used. For (A–D) data are shown for an individual experiment with four replicates per sample. The CTRL^{KO 1&2} sample was used as control for performing Dunnett's multiple comparison test for samples treated with vincristine.

p50 (*NFKB1*) transcription factors, whereas TRAF2 and TRAF3 inhibit TNFR-signalling in the non-canonical NF-κB pathway that leads to translocation of Rel-B (*RELB*) and p52 (*NFKB2*).³⁶ This suggests that for SU-DHL-5 cells, the activation of Rel-B and p52 is beneficial, whereas the activation of p65, C-Rel and p50 is not. In fact, our screening data showed that *RELB* and *NFKB2* were essential for SU-DHL-5 cells with JAKS scores for saline-treated samples on -2.6 and -1.7, respectively, whereas *RELA*, *REL* and *NFKB1* were not essential (scores on -0.1, 0.1, and -0.9, respectively). Previously, several studies have shown that GCB-subtype DLBCL cells rely primarily on BCR signalling through the PI3K-AKT-mTOR pathway, but do not depend on NF-κB signalling.^{19,50,51} However, in agreement with our results, a subset of GCB-subtype DLBCL cells have been shown to rely on NF-κB signalling through the Rel-B transcription factor.⁵²

Recently, three studies used genome-wide CRISPR screening to uncover the cellular response to centrosome loss.^{53–55}

All three studies identified USP28, p53 and 53BP1 as essential for inducing cell cycle arrest and apoptosis through p21 activation upon centrosome loss or prolonged mitosis. The three studies showed that USP28 and p53 bind to the scaffolding protein 53BP1, where USP28 de-ubiquitinates and, thus, stabilizes p53. They identified this response as a mitotic surveillance pathway independent of the SAC and the DNA damage checkpoint.⁴⁰ In addition, another study using genome-wide CRISPR screening identified the mitotic surveillance pathway as the major driver behind resistance to the antimetabolic drug TH588.⁵⁶ Furthermore, in the study by Oshima et al investigating the vincristine response in ALL, the genes *TP53*, *TP53BP1*, *USP28* and *KIF18B* ranked as number 1, 8, 15 and 368 as LOF resistance-mediating genes, respectively.¹⁵ Altogether, this suggests that USP28 and 53BP1-mediated stabilization of p53 is an important response to antimetabolic treatments.

It remains unclear how the mitotic surveillance pathway is initiated. Luessing et al showed that KIF18B binds 53BP1

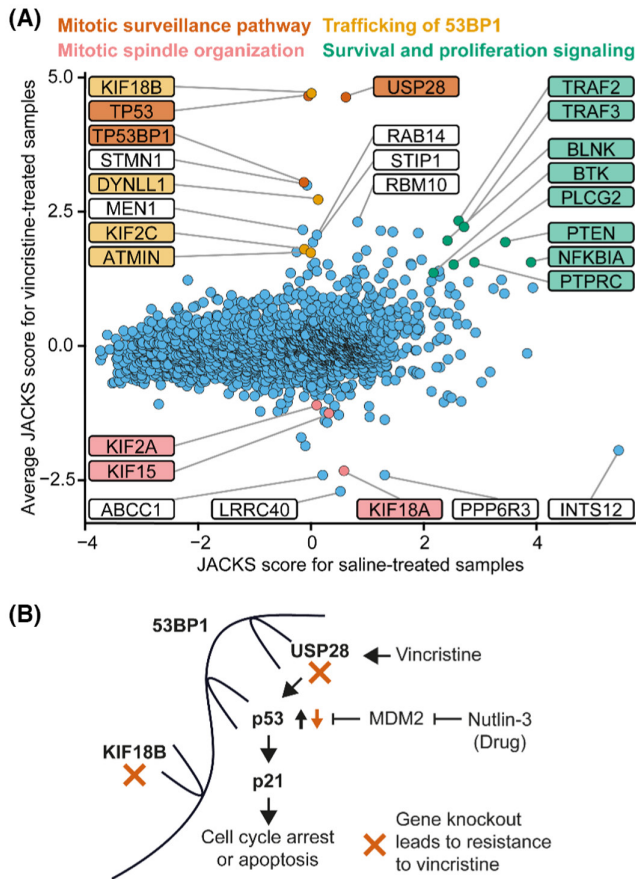


FIGURE 7 Inhibition of the mitotic surveillance pathway induces resistance to vincristine. (A) The average JAKS scores for the vincristine samples plotted against JAKS scores for the saline-treated samples. Colour-highlighted genes are connected to the mechanism indicated in the same colour above. (B) The proposed hypothesis. Vincristine induces the mitotic surveillance pathway entailing that the scaffolding protein 53BP1 binds USP28 and p53 enabling USP28 to de-ubiquitinate and thus, stabilize p53 from the ubiquitination from MDM2. The stabilized and activated p53 further activates p21 resulting in cell cycle arrest and apoptosis. KIF18B mediates this mechanism by binding and ensuring trafficking of 53BP1.

and is responsible for trafficking 53BP1 to the chromatin in response to DNA damage to mediate double-stranded DNA break repair.⁵⁷ We speculate that the stabilization of activated p53 by binding 53BP1 and USP28 is enabled by the kinesin KIF18B ensuring the trafficking of 53BP1. Thus, knockout of either *TP53*, *TP53BP1*, *USP28* or *KIF18B* disrupts the mitotic surveillance pathway by opposing the stabilization and trafficking of activated p53, resulting in less cell cycle arrest and apoptosis and, hence, increased tolerance to vincristine (Figure 7B). This would explain why the lack of *KIF18B*, but not of *USP28*, resulted in less cell cycle arrest and apoptosis for the *TP53*-mutated OCI-Ly7. As the amount of p53 protein already is high, USP28-mediated stabilization of p53 has little effect, whereas KIF18B-mediated trafficking of 53BP1 enables induction of cell cycle arrest and apoptosis by activated p53. Although this explanation remains speculative, further support is found in our screening data revealing multiple genes related to 53BP1-trafficking of

which knockout induced vincristine resistance (Figure 7A). One of the top-ranked LOF genes inducing vincristine resistance was *DYNLL1*, a member of the cytoplasmic dynein 1 complex, which is involved in intracellular trafficking along microtubules. Interestingly, *DYNLL1* also binds 53BP1,⁵⁸ and another of the top-ranked genes *ATMIN* encodes a transcription factor responsible for *DYNLL1* gene transcription.⁵⁹ Another top-ranked gene *KIF2C* encodes a kinesin-13 motor family member, which is known to be involved in trafficking along microtubules in DNA damage responses and has been shown to co-localize and co-migrate with 53BP1.⁶⁰

A recent study showed that p53 transiently localizes to centrosomes during mitosis and that inhibition of this localization leads to the accumulation of activated p53 in foci that are required for recruitment of 53BP1 to mediate the stabilization of activated p53.⁶¹ Vincristine may interfere with the localization of p53 at centrosomes either directly by interacting with the microtubular structure at the centrosome or indirectly by inducing chromosome instability, leading to misregulated centrosomes. Interestingly, clinically relevant doses of the microtubule-binding drug paclitaxel primarily exerts a cytotoxic effect by inducing chromosome instability leading to multipolar spindles and misregulated centrosomes.⁶²

It has long been suggested that a p53-dependent checkpoint controls correct mitosis in interphase.^{63,64} However, it has been unclear whether this checkpoint functions independently from the DNA damage checkpoint in interphase and from the intensification of apoptotic signalling during the SAC that pauses mitosis at metaphase.^{8,65} Notably, in our screening data knockout of genes responsible for the induction of the SAC or for recognizing DNA damage did not affect the vincristine response.

TP53 is the most frequently mutated gene in cancer and is a recurrent mutation in relapsed/refractory DLBCL.⁶⁶ In this study and in Laursen et al.,²⁹ the *TP53*-mutated cell line OCI-Ly7 was more resistant to vincristine than the *TP53* wildtype cell line SU-DHL-5. Furthermore, our study suggests that the effect of vincristine in killing cancerous cells relies on a p53 response implicating that vincristine is less effective in loss-of-function *TP53*-mutated cells.

Based on genome-wide CRISPR screens, this work identifies new DLBCL drug targets, of which small molecular inhibitors may potentially support the effect of vincristine. We find that BTB-1, an inhibitor of KIF18A, in combination with vincristine shows synergistic effects in eradicating DLBCL cells. Through this work, we also demonstrate that the dysregulation of the mitotic surveillance pathway unveils novel mechanisms supporting vincristine resistance in B-cells. Altogether, our findings contribute to a molecular understanding of resistance to vincristine in DLBCL, which may potentially support future drug development.

AUTHOR CONTRIBUTIONS

ABR, EAT, KD and JGM conceptualized the study. ABR and EAT performed the CRISPR screen. YL performed NGS.

ABR performed bioinformatics analyses. ABR, IN and TWS performed functional studies. ABR and JGM wrote the manuscript. All authors approved the final manuscript.

ACKNOWLEDGEMENTS

The authors thank FACS Core Facility, Aarhus University, Denmark for guidance and access to flow cytometers. This work was made possible through support from the following funding agencies: Independent Research Fund Denmark, The Carlsberg Foundation, NEYE-Fonden, Direktør Jacob Madsens og Olga Madsens Fond, Dagmar Marshalls Fond, Fabrikant Einar Willumsens Mindelegat, Raimond og Dagmar Ringgård-Bohns Fond, Andersen-Isted Fonden and Helga og Peter Kornings Fond.

CONFLICT OF INTEREST STATEMENT


The authors declare no conflict of interest.

ORCID

Anne Bruun Rovsing  <https://orcid.org/0000-0002-0510-180X>

Emil Aagaard Thomsen  <https://orcid.org/0000-0002-2685-7745>

Yonglun Luo  <https://orcid.org/0000-0002-0007-7759>

Jacob Giehm Mikkelsen  <https://orcid.org/0000-0002-1322-3209>

REFERENCES

- Howlader N, Noone A, Krapcho M, Miller D, Brest A, Yu M. Cancer statistics review, 1975–2016—SEER statistics. Based on November 2018 SEER data submission, posted to the SEER web site, April 2019. [Internet]. Accessed 13 October 2021. https://seer.cancer.gov/csr/1975_2016/. Available from:
- Hill BT, Kahl B. Upfront therapy for diffuse large B-cell lymphoma: looking beyond R-CHOP. *Expert Rev Hematol*. 2022;15(9):805–12.
- Tilly H, Morschhauser F, Sehn LH, Friedberg JW, Trněný M, Sharman JP, et al. Polatumumab vedotin in previously untreated diffuse large B-cell lymphoma. *N Engl J Med*. 2022;386(4):351–63.
- Schmitz R, Wright GW, Huang DW, Johnson CA, Phelan JD, Wang JQ, et al. Genetics and pathogenesis of diffuse large B-cell lymphoma. *N Engl J Med*. 2018;378(15):1396–407.
- Chapuy B, Stewart C, Dunford AJ, Kim J, Kamburov A, Redd RA, et al. Molecular subtypes of diffuse large B cell lymphoma are associated with distinct pathogenic mechanisms and outcomes. *Nat Med*. 2018;24(5):679–90.
- Lacy SE, Barrans SL, Beer P, Painter D, Smith A, Roman E, et al. Targeted sequencing in DLBCL, molecular subtypes, and outcomes: a haematological malignancy research network report. *Blood*. 2020;135(20):1759–71.
- DeVita VT, Chu E. A history of cancer chemotherapy. *Cancer Res*. 2008;68(21):8643–53.
- Shi J, Mitchison TJ, Shi J, Mitchison TJ. Cell death response to anti-mitotic drug treatment in cell culture, mouse tumor model and the clinic. *Endocr Relat Cancer*. 2017;24(9):T83–96.
- Matthews HK, Bertoli C, de Bruin RAM. Cell cycle control in cancer. *Nat Rev Mol Cell Biol*. 2021;23(1):74–88.
- Shalem O, Sanjana NE, Hartenian E, Shi X, Scott DA, Mikkelsen TS, et al. Genome-scale CRISPR-Cas9 knockout screening in human cells. *Science*. 2014;343(6166):84–7.
- Wang T, Wei JJ, Sabatini DM, Lander ES. Genetic screens in human cells using the CRISPR-Cas9 system. *Science*. 2014;343(6166):80–4.
- Koike-Yusa H, Li Y, Tan EP, Velasco-Herrera MDC, Yusa K. Genome-wide recessive genetic screening in mammalian cells with a lentiviral CRISPR-guide RNA library. *Nat Biotechnol*. 2014;32(3):267–73.
- Thomsen EA, Røvsing AB, Anderson MV, Due H, Huang J, Luo Y, et al. Identification of BLNK and BTK as mediators of rituximab-induced programmed cell death by CRISPR screens in GCB-subtype diffuse large B-cell lymphoma. *Mol Oncol*. 2020;14:1978–97.
- Palmer AC, Chidley C, Sorger PK. A curative combination cancer therapy achieves high fractional cell killing through low cross resistance and drug additivity. *elife*. 2019;1:8.
- Oshima K, Zhao J, Pérez-Durán P, Brown JA, Patiño-Galindo JA, Chu T, et al. Mutational and functional genetics mapping of chemotherapy resistance mechanisms in relapsed acute lymphoblastic leukemia. *Nat Cancer*. 2020 Oct 19;1(11):1113–27.
- Mo Z, Wood S, Namiranian S, Mizukoshi R, Weng S, Jang IS, et al. Deciphering the mechanisms of CC-122 resistance in DLBCL via a genome-wide CRISPR screen. *Blood Adv*. 2021;5(7):2027–39.
- Tong KI, Yoon S, Isaev K, Bakhtiari M, Lackraj T, He MY, et al. Combined EZH2 inhibition and IKAROS degradation leads to enhanced antitumor activity in diffuse large B-cell lymphoma. *Clin Cancer Res*. 2021 Oct 1;27(19):5401–14.
- Reddy A, Zhang J, Davis NS, Moffitt AB, Love CL, Waldrop A, et al. Genetic and functional drivers of diffuse large B cell lymphoma. *Cell*. 2017;171(2):481–494.e15.
- Phelan JD, Young RM, Webster DE, Roulland S, Wright GW, Kasbekar M, et al. A multiprotein supercomplex controlling oncogenic signaling in lymphoma. *Nature*. 2018;560(7718):387–91.
- Nie M, Du L, Ren W, Joung J, Ye X, Shi X, et al. Genome-wide CRISPR screens reveal synthetic lethal interaction between CREBBP and EP300 in diffuse large B-cell lymphoma. *Cell Death Dis*. 2021;12(5):419.
- Locke J, Joseph AP, Peña A, Möckel MM, Mayer TU, Topf M, et al. Structural basis of human kinesin-8 function and inhibition. *Proc Natl Acad Sci USA*. 2017;114(45):E9539–48.
- Ryø LB, Thomsen EA, Mikkelsen JG. Production and validation of lentiviral vectors for CRISPR/Cas9 delivery. *Methods Mol Biol*. 2019;1961:93–109.
- Thomsen EA, Mikkelsen JG. CRISPR-based lentiviral knockout libraries for functional genomic screening and identification of phenotype-related genes. *Methods Mol Biol*. 2019;1961:343–57.
- Hart T, Brown KR, Sircoulomb F, Rottapel R, Moffat J. Measuring error rates in genomic perturbation screens: gold standards for human functional genomics. *Mol Syst Biol*. 2014;10(7):733.
- Allen F, Behan F, Khodak A, Iorio F, Yusa K, Garnett M, et al. JACKS: joint analysis of CRISPR/Cas9 knock-out screens. *Genome Res*. 2019;29(3):464–71.
- Ge SX, Jung D, Jung D, Yao R. ShinyGO: a graphical gene-set enrichment tool for animals and plants. *Bioinformatics*. 2020;36(8):2628–9.
- Yang L, Chen R, Goodison S, Sun Y. An efficient and effective method to identify significantly perturbed subnetworks in cancer. *Nat Comput Sci*. 2021;1(1):79–88.
- Clement K, Rees H, Canver MC, Gehrke JM, Farouni R, Hsu JY, et al. CRISPResso2 provides accurate and rapid genome editing sequence analysis. *Nat Biotechnol*. 2019;37(3):224–6.
- Laursen MB, Falgreen S, Bødker JS, Schmitz A, Kjeldsen MK, Sørensen S, et al. Human B-cell cancer cell lines as a preclinical model for studies of drug effect in diffuse large B-cell lymphoma and multiple myeloma. *Exp Hematol*. 2014;42(11):927–38.
- Doench JG, Fusi N, Sullender M, Hegde M, Vaimberg EW, Donovan KF, et al. Optimized sgRNA design to maximize activity and minimize off-target effects of CRISPR-Cas9. *Nat Biotechnol*. 2016;34(2):184–91.
- Falgreen S, Dybkær K, Young KH, Xu-Monette ZY, El-Galaly TC, Laursen MB, et al. Predicting response to multidrug regimens in cancer patients using cell line experiments and regularised regression models. *BMC Cancer*. 2015;15(1):1–15.

32. Li W, Köster J, Xu H, Chen CH, Xiao T, Liu JS, et al. Quality control, modeling, and visualization of CRISPR screens with MAGeCK-VISPR. *Genome Biol.* 2015;16(1):1–13.
33. Cole SPC. Targeting multidrug resistance protein 1 (MRP1, ABCC1): past, present, and future. *Annu Rev Pharmacol Toxicol.* 2014;54:95–117.
34. Eustermann S, Schall K, Di K, Lakomek K, Strauss M, Moldt M, et al. Structural basis for ATP-dependent chromatin remodelling by the INO80 complex. *Nature.* 2018;556(7701):386–90.
35. Liu GY, Sabatini DM. mTOR at the nexus of nutrition, growth, ageing and disease. *Nat Rev Mol Cell Biol.* 2020;21(4):183–203.
36. Pasqualucci L, Klein U. NF- κ B mutations in germinal center B-cell lymphomas: relation to NF- κ B function in Normal B cells. *Biomedicines.* 2022;10(10):2450.
37. Weaver LN, Ems-McClung SC, Stout JR, Leblanc C, Shaw SL, Gardner MK, et al. Kif18A uses a microtubule binding site in the tail for plus-end localization and spindle length regulation. *Curr Biol.* 2011;21(17):1500–6.
38. McHugh T, Gluszek AA, Welburn JPI. Microtubule end tethering of a processive kinesin-8 motor Kif18b is required for spindle positioning. *J Cell Biol.* 2018;217(7):2403–16.
39. Wang X, Liu Z, Zhang L, Yang Z, Chen X, Luo J, et al. Targeting deubiquitinase USP28 for cancer therapy. *Cell Death Dis.* 2018;9(2):1–10.
40. Lambrus BG, Holland AJ. A new mode of mitotic surveillance. *Trends Cell Biol.* 2017 May 1;27(5):314–21.
41. Joerger AC, Ang HC, Fersht AR. Structural basis for understanding oncogenic p53 mutations and designing rescue drugs. *Proc Natl Acad Sci USA.* 2006 Oct 10;103(41):15056–61.
42. Lahav G, Rosenfeld N, Sigal A, Geva-Zatorsky N, Levine AJ, Elowitz MB, et al. Dynamics of the p53-Mdm2 feedback loop in individual cells. *Nat Genet.* 2004;36(2):147–50.
43. Vassilev LT, Vu BT, Graves B, Carvajal D, Podlaski F, Filipovic Z, et al. In vivo activation of the p53 pathway by small-molecule antagonists of MDM2. *Science.* 2004 Feb 6;303(5659):844–8.
44. Stewart ZA, Tang LJ, Pietenpol JA. Increased p53 phosphorylation after microtubule disruption is mediated in a microtubule inhibitor- and cell-specific manner. *Oncogene.* 2001;20(1):113–24.
45. Spinner MA, Aleshin A, Santaguida MT, Schaffert SA, Zehnder JL, Patterson AS, et al. Ex vivo drug screening defines novel drug sensitivity patterns for informing personalized therapy in myeloid neoplasms. *Blood Adv.* 2020;4(12):2768–78.
46. Goh J, De Mel S, Hoppe MM, Mohd Abdul Rashid MB, Zhang XY, Jaynes P, et al. An ex vivo platform to guide drug combination treatment in relapsed/refractory lymphoma. *Sci Transl Med.* 2022;14(667):eabn7824.
47. Sturgill EG, Ohi R. Kinesin-12 differentially affects spindle assembly depending on its microtubule substrate. *Curr Biol.* 2013;23(14):1280–90.
48. Uehara R, Tsukada Y, Kamasaki T, Poser I, Yoda K, Gerlich DW, et al. Aurora B and Kif2A control microtubule length for assembly of a functional central spindle during anaphase. *J Cell Biol.* 2013;202(4):623–36.
49. Cohen-Sharir Y, McFarland JM, Abdusamad M, Marquis C, Bernhard SV, Kazachkova M, et al. Aneuploidy renders cancer cells vulnerable to mitotic checkpoint inhibition. *Nature.* 2021;590(7846):486–91.
50. Eric Davis R, Brown KD, Siebenlist U, Staudt LM. Constitutive nuclear factor κ B activity is required for survival of activated B cell-like diffuse large B cell lymphoma cells. *J Exp Med.* 2001;194(12):1861–74.
51. Havranek O, Xu J, Köhrer S, Wang Z, Becker L, Comer JM, et al. Tonic B-cell receptor signaling in diffuse large B-cell lymphoma. *Blood.* 2017;130(8):995–1006.
52. Eluard B, Nuan-Aliman S, Faumont N, Collares D, Bordereaux D, Montagne A, et al. The alternative RelB NF- κ B subunit is a novel critical player in diffuse large B-cell lymphoma. *Blood.* 2022;139(3):384–98.
53. Lambrus BG, Daggubati V, Uetake Y, Scott PM, Clutario KM, Sluder G, et al. A USP28–53BP1–p53–p21 signaling axis arrests growth after centrosome loss or prolonged mitosis. *J Cell Biol.* 2016;214(2):143–53.
54. Fong CS, Mazo G, Das T, Goodman J, Kim M, O'Rourke BP, et al. 53BP1 and USP28 mediate p53-dependent cell cycle arrest in response to centrosome loss and prolonged mitosis. *elife.* 2016;2:5.
55. Meitinger F, Anzola JV, Kaulich M, Richardson A, Stender JD, Benner C, et al. 53BP1 and USP28 mediate p53 activation and G1 arrest after centrosome loss or extended mitotic duration. *J Cell Biol.* 2016;214(2):155–66.
56. Gul N, Karlsson J, Tängemo C, Linsefors S, Tuyizere S, Perkins R, et al. The MTH1 inhibitor TH588 is a microtubule-modulating agent that eliminates cancer cells by activating the mitotic surveillance pathway. *Sci Rep.* 2019;9(1):1–12.
57. Luessing J, Sakhteh M, Sarai N, Frizzell L, Tsanov N, Ramberg KO, et al. The nuclear kinesin KIF18B promotes 53BP1-mediated DNA double-strand break repair. *Cell Rep.* 2021;35(13):109306.
58. Becker JR, Cuella-Martin R, Barazas M, Liu R, Oliveira C, Oliver AW, et al. The ASCIZ-DYNLL1 axis promotes 53BP1-dependent non-homologous end joining and PARP inhibitor sensitivity. *Nat Commun.* 2018;9(1):1–12.
59. Jurado S, Conlan LA, Baker EK, Ng JL, Tennis N, Hoch NC, et al. ATM substrate Chk2-interacting Zn²⁺ finger (ASCIZ) is a Bi-functional transcriptional activator and feedback sensor in the regulation of dynein light chain (DYNLL1) expression. *J Biol Chem.* 2012;287(5):3156–64.
60. Zhu S, Paydar M, Wang F, Li Y, Wang L, Barrette B, et al. Kinesin Kif2C in regulation of DNA double strand break dynamics and repair. *elife.* 2020;9:9.
61. Contadini C, Monteonofrio L, Virdia I, Prodosmo A, Valente D, Chessa L, et al. p53 mitotic centrosome localization preserves centrosome integrity and works as sensor for the mitotic surveillance pathway. *Cell Death Dis.* 2019;10(11):1–16.
62. Zasadil LM, Andersen KA, Yeum D, Rocque GB, Wilke LG, Tevaarwerk AJ, et al. Cytotoxicity of paclitaxel in breast cancer is due to chromosome missegregation on multipolar spindles. *Sci Transl Med.* 2014;6(229):229ra43.
63. Cross SM, Sanchez CA, Morgan CA, Schimke MK, Ramel S, Idzerda RL, et al. A p53-dependent mouse spindle checkpoint. *Science.* 1995;267(5202):1353–6.
64. Lanni JS, Jacks T. Characterization of the p53-dependent postmitotic checkpoint following spindle disruption. *Mol Cell Biol.* 1998 Feb;18(2):1055–64.
65. Gascoigne KE, Taylor SS. Cancer cells display profound intra- and interline variation following prolonged exposure to antimetabolic drugs. *Cancer Cell.* 2008;14(2):111–22.
66. Morin RD, Assouline S, Alcaide M, Mohajeri A, Johnston RL, Chong L, et al. Genetic landscapes of relapsed and refractory diffuse large B-cell lymphomas. *Clin Cancer Res.* 2016;22(9):2290–300.

SUPPORTING INFORMATION

Additional supporting information can be found online in the Supporting Information section at the end of this article.

How to cite this article: Rovsing AB, Thomsen EA, Nielsen I, Skov TW, Luo Y, Dybkær K, et al. Resistance to vincristine in DLBCL by disruption of p53-induced cell cycle arrest and apoptosis mediated by KIF18B and USP28. *Br J Haematol.* 2023;202(4): 825–839. <https://doi.org/10.1111/bjh.18872>